

# Fabrication and characterization of piezoresistive flexible pressure sensors based on poly(vinylidene fluoride)/thermoplastic polyurethane filled with carbon black-polypyrrole

Mayara C. Bertolini<sup>1,2</sup>  | Sithiprumnea Dul<sup>1</sup>  | Elaine C. Lopes Pereira<sup>3</sup>  |  
Bluma G. Soares<sup>3</sup>  | Guilherme M. O. Barra<sup>2</sup>  | Alessandro Pegoretti<sup>1,4</sup> 

<sup>1</sup>Department of Industrial Engineering, University of Trento, Trento, Italy

<sup>2</sup>Department of Mechanical Engineering, Universidade Federal de Santa Catarina, Florianópolis, Brazil

<sup>3</sup>Department of Metallurgical and Material Engineering, Universidade Federal do Rio de Janeiro, Centro de Tecnologia, Rio de Janeiro, Brazil

<sup>4</sup>National Interuniversity Consortium of Materials Science and Technology (INSTM), Florence, Italy

## Correspondence

Mayara C. Bertolini, Department of Industrial Engineering, University of Trento, Trento, Italy.  
Email: mayara.bertolini@unitn.it

## Funding information

Italian Ministry for University and Research (MUR), Grant/Award Number: L.232/2016

## Abstract

Electrically conductive composites of thermoplastic polyurethane (TPU), poly(vinylidene fluoride) (PVDF), and carbon black-polypyrrole (CB-PPy) were prepared by melt compounding followed by compression molding or by filament production followed by fused filament fabrication (FFF). The storage modulus ( $G'$ ) and complex viscosity ( $\eta^*$ ) of the composites increased with the addition of CB-PPy leading to a more rigid material. The electrical and rheological percolation threshold of composites were 5 and 3 wt%, respectively. In fact, composites with 5 wt% or more CB-PPy content display  $G'$  higher than  $G''$  indicating a solid-like behavior. Furthermore, the addition of CB-PPy increased the electrical conductivity of all composites. However, the electrical conductivity values of composites containing 5 and 6 wt% of CB-PPy produced by compression molding are one and seven order of magnitude higher than those of FFF composites with same composition. Compression molded and 3D printed composites with 6 wt% of CB-PPy displayed high sensitivity/gauge factor, large measurement range and reproducible piezoresistive response during 100 loading-unloading cycles for both processing methods. The results presented in this study demonstrated the potential use of FFF for producing piezoresistive flexible sensors based on PVDF/TPU/CB-PPy composites.

## KEYWORDS

compression molding, conductive polymeric composites, fused filament fabrication, piezoresistive sensors, polymer blends, pressure sensors

## 1 | INTRODUCTION

Flexible and highly sensitive pressure sensors have been widely studied for various applications in soft

robotics, wearable electronics, such as human-machine interface and electronic skin, and prosthetics.<sup>1,2</sup> One of the most interesting type of pressure sensors are piezoresistive sensors, which are able to change their

This is an open access article under the terms of the Creative Commons Attribution-NonCommercial-NoDerivs License, which permits use and distribution in any medium, provided the original work is properly cited, the use is non-commercial and no modifications or adaptations are made.

© 2021 The Authors. *Polymer Composites* published by Wiley Periodicals LLC on behalf of Society of Plastics Engineers.

electrical resistivity in response to applied compressive forces.<sup>2-5</sup> Piezoresistive sensors are broadly studied for pressure sensing due to their simple device structure, broad range of detection, easy read-out mechanism, low energy consumption, high linearity and easy fabrication.<sup>5,6</sup>

Piezoresistive pressure sensors based on conductive polymeric composites (CPC) have been widely reported for their good processability, low cost, fast and linear response, and reproducibility.<sup>4,7-9</sup> They are usually prepared by the addition of electrically conductive fillers into insulating polymeric matrices.<sup>3,10</sup> Combining characteristics of insulating matrix and conductive filler is a great advantage in the production of CPC to produce pressure sensors due to its superior properties when compared to the neat components.<sup>2,4</sup>

The response of piezoresistive pressure sensors under cyclic loading conditions depends on the compressive or tensile forces applied and the temperature.<sup>2,3,5,11-13</sup> In fact, when in the undeformed state, the composite consists of conductive particles dispersed in an insulating polymeric matrix and its electrical conductivity is limited by the low conductivity of the insulating matrix. The application of a compressive force induces an elastic deformation of the matrix, decreasing the distance between the conductive particles of the filler until they approach each other thus increasing the composite electrical conductivity. However, when the compressive force is released, the composite returns to its undeformed shape and the initial electrical conductivity is restored.<sup>2,3,8,11-13</sup> Nevertheless, during the cyclic loading the conductive network of the filler can be irreversibly modified and hysteresis effects might be observed after repeated loading-unloading cycles, which is also related to the polymers viscoelasticity and interaction between components of the mixture.<sup>3,6,9,14</sup>

The main challenge in the development of sensors based on CPCs is achieving good responses at minimum filler concentration to maintain the mechanical properties and processability of the matrix.<sup>12</sup> Some researchers report the preparation of polymer blends to reduce the percolation threshold due to the preferable localization of the conductive filler in one phase or at the interface between the phases of the blend.<sup>8,9,15-25</sup> In fact, the final properties and sensitivity of sensors based on CPC rely not only on the filler concentration and the intrinsic properties of polymers and fillers (for instance, electrical conductivity, thermal properties, degree of crystallinity, miscibility, etc.), but also on the interaction between them, the type of conductive network and the dispersion and distribution of filler. The performance of the piezoresistive sensor can be quantified by the gauge factor and the sensitivity of the sensor that are related to sensor

ability and accuracy in converting the external stimulus into electrical signals associated to the piezoresistive intrinsic effect and geometry factors.<sup>4-6</sup>

Moreover, the processing method and testing parameters play a significant role on the final properties of the sensor.<sup>2-4,12</sup> Although preparation methods such as solution casting, electrospinning, in situ polymerization are used to produce materials with good sensing performance, a facile fabrication method for industrial-scale production is still a challenge.<sup>4,10,26</sup> In this framework, a promising technology for fabrication of flexible pressure sensors is additive manufacturing (AM), also called 3D printing, via fused filament fabrication (FFF), which offers the advantages of low cost, versatility and large scale production.<sup>1,5,27</sup> Some studies show the advantages of preparing electronic devices via FFF composed of CPCs that are able to detect electrical conductive variations under flexure, strain and compressive forces.<sup>1,10,28,29</sup> Ahmed et al<sup>28</sup> prepared polymeric composites of poly(methyl methacrylate)/carbon nanotubes (PMMA/CNT) by FFF for flexible electronic devices evaluating the mechanical, thermal and electrical properties of the composite. Leigh et al<sup>29</sup> studied the fabrication of capacitive and piezoresistive sensors of polycaprolactone/carbon black (PCL/CB) using the FFF technique. Moreover, Alsharari et al<sup>1</sup> investigated the electrical conductivity variation with the applied strain for polylactic acid/thermoplastic polyurethane/graphene (PLA/TPU/GR) composites. Combining the FFF technique with CPC is an efficient way to fabricate materials with conductive, structural and sensor functionalities.<sup>4,26,30</sup> Several studies report the preparation of electromechanical sensors by FFF technique,<sup>1,10,26,28-30</sup> however, only a few are used as piezoresistive pressure sensor<sup>30</sup> and strain sensor.<sup>31,32</sup> Furthermore, only a few studies report on the use of polymeric blends to control properties and improve printability of composite filaments for FFF.<sup>24,33</sup>

Our previous work focused on the development of flexible and highly conductive filaments composed of polymeric blends of poly(vinylidene fluoride) (PVDF) and TPU in order to achieve the best relationship between mechanical properties, electrical conductivity and printability. Two polymeric blends composed of PVDF/TPU were used as matrix to prepared compression molded and 3D printed composites comprising carbon black-polypyrrole (CB-PPy) as conductive filler. The results showed that the investigated PVDF/TPU/CB-PPy composites can be potentially used for technological applications that requires electrical conductivity.<sup>33</sup>

In this context, the present study focuses on the use of the previous developed materials as flexible pressure sensors. Due to the good combination of flexibility,

printability and electrical properties, the composites prepared in the mentioned research comprising PVDF/TPU 50/50 wt% as matrix are further characterized in this paper and their piezoresistive response are investigated to evaluate its application as piezoresistive flexible pressure sensors.

## 2 | EXPERIMENTAL

### 2.1 | Materials

The polymers used in this study were a PVDF, Amboflon PVDF-24 from Amboflon GmbH (Hamburg, Germany) and a TPU, Desmopan DP 6064 A from Covestro Italia srl (Milano, Italy). The conductive filler was carbon black doped with 20 wt% of polypyrrole (CB-PPy) purchased from Sigma Aldrich. Some properties of these materials are reported in Table 1.

### 2.2 | Sample preparation

#### 2.2.1 | Preparation of PVDF/TPU/CB-PPy composites

The composites were based on a PVDF/TPU blend composed of 50/50 wt% of each polymer. They were prepared by melt compounding using a Thermo-Haake PolyLab Rheomix 600 internal mixer with an internal volume of 50 cm<sup>3</sup> equipped with counter-rotating rotors. All materials were dried overnight at 60°C. PVDF and TPU were mixed for 2 min at 180°C and a rotor speed of 50 rpm. Then, CB-PPy was added in the mixing chamber in the compositions shown in Table 2 and mixed for 13 more minutes.

#### 2.2.2 | Compression molding

The mixtures described in Table 2 were compression molded in a Carver Laboratory press (Carver, Inc. Wabash,

IN) at 180°C for 10 min under a pressure of 3.9 MPa to obtain square plates of 12 mm<sup>2</sup> with 2 mm thickness.

#### 2.2.3 | Preparation of filaments

The composites containing 5 and 6 wt% of CB-PPy were selected to be printed via FFF due to their good electrical conductivity. After melt compounding the composites were grinded and extruded in filaments with a final diameter of 1.75 mm ± 0.10 mm. A single screw extruder Friul Filiere SpA, model Estru 13 was used for the filaments production operating at 30 rpm with four temperature zones of 130, 170, 175 and 180°C (die).

#### 2.2.4 | Fused filament fabrication

The filaments were printed by a Sethi S3 3D printer, via FFF. As depicted in Figure 1, the samples were printed in circular disks with a diameter of 15 mm and a thickness of 2 mm, and the layers were deposited along horizontal alternate direction (H45). The specimen was drawn using AutoCAD and sliced using the open-source software Slic3r. The printing parameters adopted for the FFF process are summarized in Table 3.

**TABLE 2** Composition of the investigated PVDF/TPU/CB-PPy composites

PVDF/TPU wt %	CB-PPy wt%
100	0
97	3
95	5
94	6
93	7
90	10
85	15

Abbreviations: CB-PPy, carbon black-polypyrrole; PVDF, poly(vinylidene fluoride); TPU, thermoplastic polyurethane.

**TABLE 1** Properties of PVDF, TPU and CB-PPy

Material	Melting temperature $T_m$ (°C)	Glass transition temperature $T_g$ (°C)	Density ( $\text{g}\cdot\text{cm}^{-3}$ )	Electrical conductivity ( $\text{S}\cdot\text{m}^{-1}$ )
PVDF	165–175 <sup>a</sup>	–39.2 <sup>33</sup>	1.78 <sup>a</sup>	$10^{-13}$ <sup>33</sup>
TPU	200–220 <sup>a</sup>	–25 <sup>33</sup>	1.09 <sup>a</sup>	$10^{-11}$ <sup>33</sup>
CB-PPy	-	-	2.22 <sup>b</sup>	$3 \times 10^{1a}$

Abbreviations: CB-PPy, carbon black-polypyrrole; PVDF, poly(vinylidene fluoride); TPU, thermoplastic polyurethane.

<sup>a</sup>Data from technical datasheet.

<sup>b</sup>Data from gas pycnometry measurement.

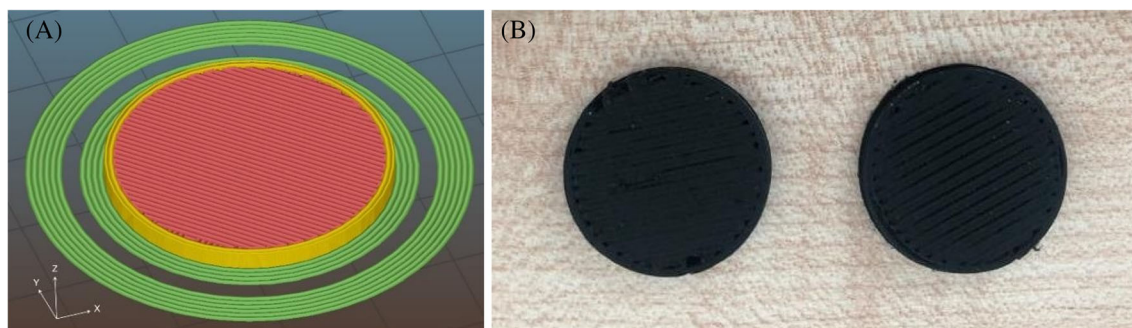


FIGURE 1 (A) Schematic representation of circular specimen and (B) a picture of 3D printed parts

TABLE 3 FFF printing parameters

Parameter	Value
Nozzle temperature	230°C
Bed temperature	40°C
Nozzle diameter	0.4 mm
Nozzle speed	40 mm.s <sup>-1</sup>
Layer height	0.2 mm
Number of layers	10
Raster angle	+45°/-45°
Infill type and density	Rectangular 100%

Abbreviation: FFF, fused filament fabrication.

### 2.3 | Testing techniques

The rheology measurements were performed using a Discovery DHR 1 rheometer from TA Instrument, Inc. in oscillatory mode using parallel plates with diameter of 25 mm and a gap of 1.0 mm for sample with filler content lower than 10% and 1.2 mm for samples with 10% of filler content. The analysis was carried out at 180°C under nitrogen atmosphere, in the frequency range from 0.1 to 100 Hz at a strain amplitude of 0.1% (linear viscoelastic region).

Scanning electron microscopy (SEM) was carried out to investigate the morphology of the compression molded and 3D printed conductive composites and dispersion and distribution of CB-PPy in the PVDF/TPU polymeric matrix. The analysis was performed on the fracture surfaces of the samples at an acceleration voltage of 5.0 kV using a Tescan VEGA3 field emission scanning electron microscope.

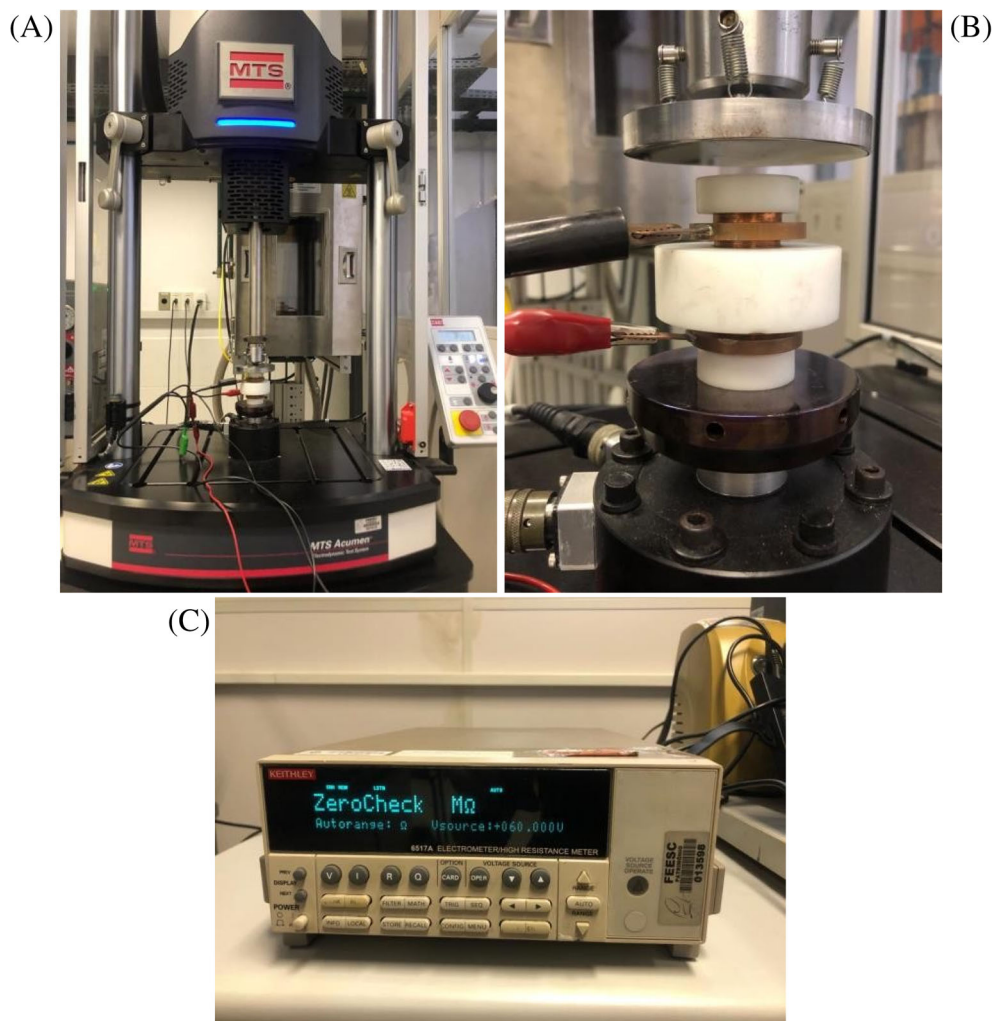
A two-probe standard method was used for measuring the electrical conductivity of high resistive samples with 2 mm of thickness. The analysis was carried out on both sides of the samples by a Keithley 6517A electrometer connected to a Keithley 8009 resistivity test fixture. On the other hand, an ASTM D4496-4 four-probe method was

performed for the high conductive samples using a DC power supply by ISO-TECH IPS303DD as voltage source and a pocket multimeter ISO-TECH IDM 67 to measure the current flow. Three samples of  $30 \times 5 \times 2 \text{ mm}^3$  were measured on both side with internal electrode of 3.69 mm.

Dynamic mechanical thermal analysis (DMTA) was performed to evaluate the storage modulus ( $E'$ ) and loss modulus ( $E''$ ) and  $\tan \delta$  as function of temperature. The glass transition temperature ( $T_g$ ) values were calculated for the composites comprising various amount of CB-PPy. The analysis was carried out from  $-80$  to  $100^\circ\text{C}$  at 1 Hz and a heating rate of  $3^\circ\text{C min}^{-1}$  under a maximum dynamic strain of 50 microns using a Netzsch DMA 242 E (Netzsch, Germany) equipment under tensile mode. Rectangular specimens of  $10 \times 5 \times 2 \text{ mm}$  were tested.

The piezoresistive behavior was evaluated by simultaneously applying controlled loads and measuring the electrical resistivity. Loading-unloading cycles were performed with a MTS Acumen universal testing machine by MTS Eden Prairie MN (Figure 2A) equipped with a load cell of 0.5 kN. Concurrently, the specimen resistance was measured by a Keithley 6517A electrometer (Figure 2B) using an in-house developed software. First, the disks specimens of 15 mm diameter were placed between two copper electrodes (Figure 2C) and the assembly located inside an electrically insulated chamber where three different maximum loads of 100, 200 and 400 N corresponding to maximum compressive pressures of 0.57, 1.14 and 2.28 MPa were applied at a loading rate of  $3.4 \text{ MPa.min}^{-1}$  to evaluate the optimal electrical response. Due to the better responses, the pressure of 2.28 MPa was selected to test the samples. The tests were firstly performed applying 2.28 MPa of compressive pressure at a rate of  $3.4 \text{ MPa.min}^{-1}$  and then the pressure was released at the same rate during five loading-unloading cycles. The samples that showed good response and reproducibility of the results were further tested under 100 loading-unloading cycles under the same conditions. The analysis was carried out for all compression molded composites and 3D printed composites. The resistivity  $\rho$

FIGURE 2 Images of (A) MTS universal testing machine, (B) device composed of two electrodes used to measure the samples resistance and (C) Keithley electrometer



( $\Omega$  cm) of the samples was calculated according to Equation (1):

$$\rho = R \frac{\pi d^2}{4w} \quad (1)$$

where  $R$  is the electrical resistance ( $\Omega$ ),  $d$  is the diameter (cm) and  $w$  is the thickness (cm) of the specimens.

### 3 | RESULTS AND DISCUSSION

#### 3.1 | Rheological analysis

Rheology studies are useful to evaluate polymer systems in order to understand the interactions between the components of a polymeric blend, as well as the dispersion and formation of a three dimensional network of the filler in the matrix.<sup>17,18,34</sup> In order to investigate the structural changes in the polymeric composites, rheological analysis was carried out in the molten state for neat

PVDF, neat TPU, PVDF/TPU 50/50 wt% and PVDF/TPU/CB-PPy composites with various filler content. The storage modulus ( $G'$ ) curves as function of frequency for neat PVDF, neat TPU and PVDF/TPU are displayed in Figure 3A and the dependence of complex viscosity ( $\eta^*$ ) with frequency in Figure 3B. The results show that TPU has higher viscosity than PVDF, while the blend PVDF/TPU presents an intermediate viscosity between the two pure components. The same occurs for the storage modulus. Figure 4 shows the storage and loss modulus vs. frequency for the neat polymers and the blend PVDF/TPU. For neat PVDF and TPU,  $G'$  is higher than the loss modulus ( $G''$ ) at low frequencies describing a solid-like behavior. However,  $G'$  and  $G''$  curves are intercepted at a specific frequency where  $G''$  becomes higher than  $G'$  indicating a liquid-like behavior. On the other hand, the blend PVDF/TPU presents  $G'' > G'$  in the low frequency range, which indicates a good interaction between PVDF and TPU.

Furthermore, the curves of storage modulus and complex viscosity as a function of frequency for PVDF/

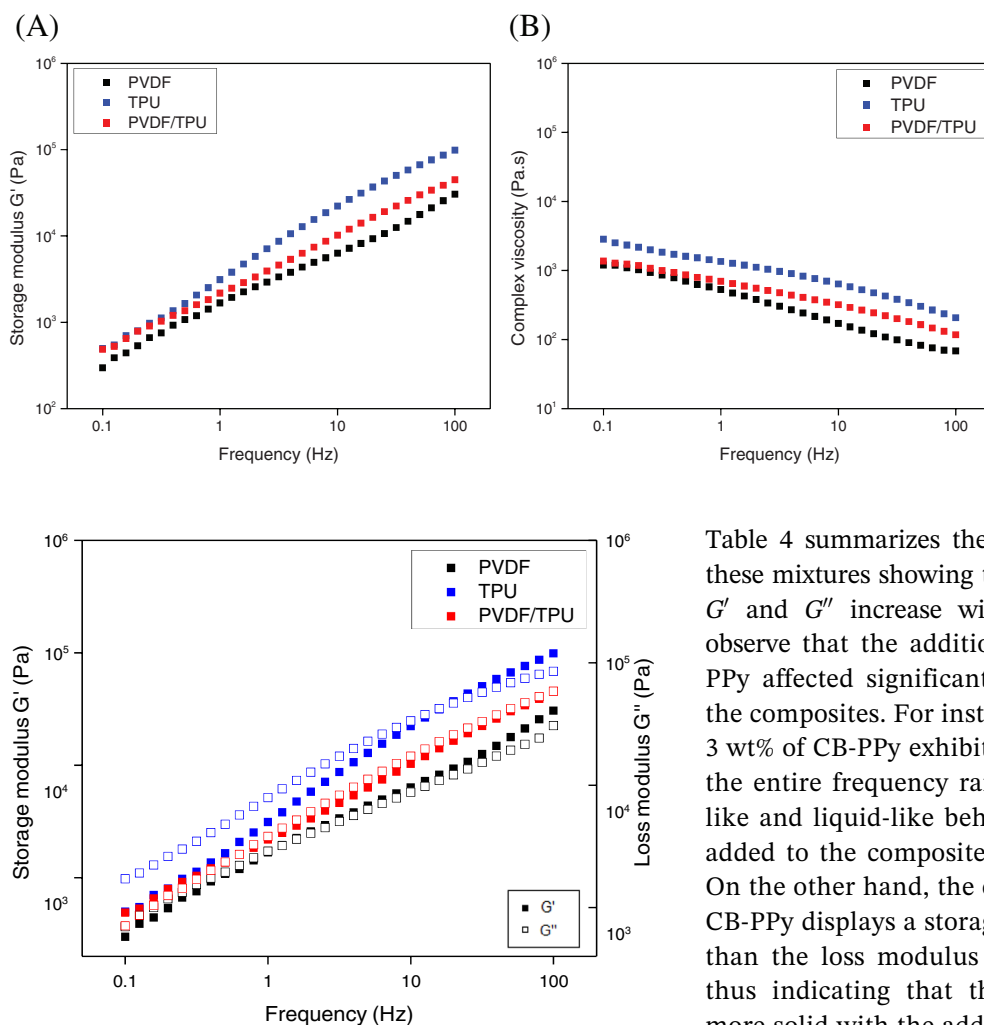


**FIGURE 3** (A) Storage modulus and (B) complex viscosity as function of temperature for neat PVDF, neat TPU and PVDF/TPU. PVDF, poly(vinylidene fluoride); TPU, thermoplastic polyurethane

**FIGURE 4** Dependence of storage and loss modulus with frequency as function of temperature for PVDF, neat TPU and PVDF/TPU. PVDF, poly(vinylidene fluoride); TPU, thermoplastic polyurethane

TPU/CB-PPy conductive composites are presented in Figure 5A,B, respectively. In Figure 5A, it is possible to observe that the storage modulus ( $G'$ ) significantly increases as the CB-PPy concentration is increased. The same behavior occurs with the complex viscosity ( $\eta^*$ ), Figure 5B, thus indicating that the addition of filler reduces the mobility of the polymer chains and increases the viscosity of the mixtures due to the formation of a 3D network. The addition of high amount of filler (i.e., 5 and 10 wt%) leads to an abrupt drop in the complex viscosity with increasing the frequency thus indicating a shear thinning behavior characteristic of the pseudo-plastic behavior.

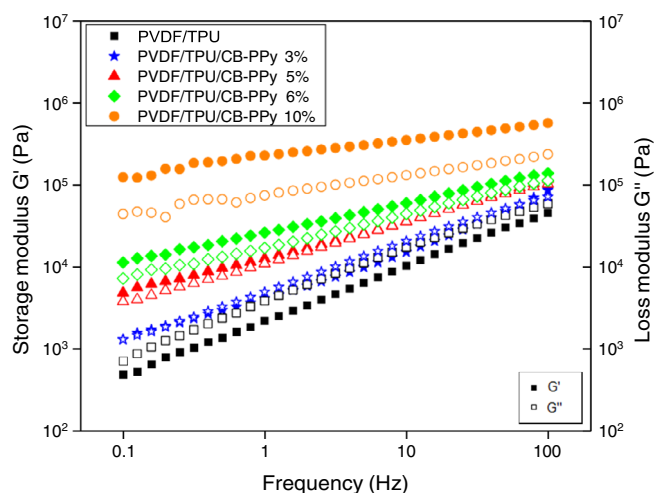
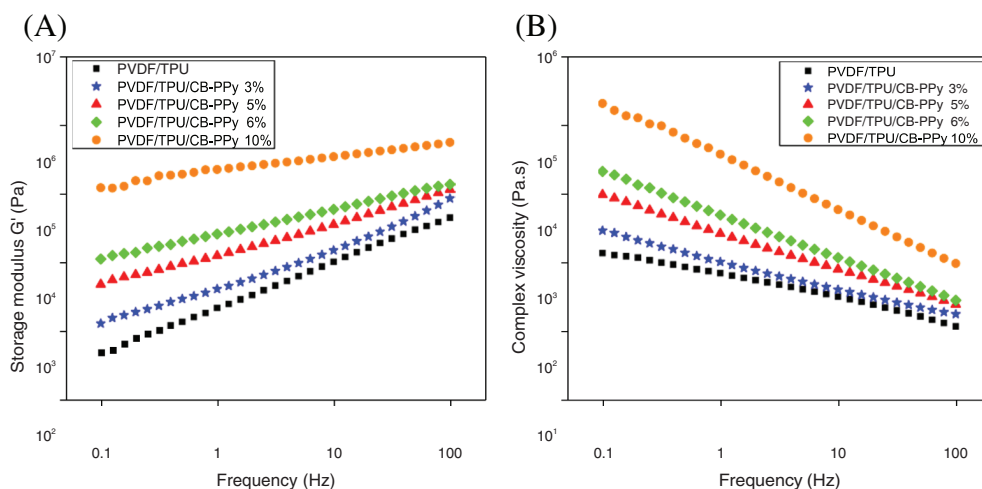
Figure 6 compares the storage ( $G'$ ) and loss ( $G''$ ) modulus profiles of PVDF/TPU/CB-PPy composites and

Table 4 summarizes the main rheological properties of these mixtures showing that for all samples the values of  $G'$  and  $G''$  increase with frequency. It is possible to observe that the addition of the conductive filler CB-PPy affected significantly the rheological behavior of the composites. For instance, the composite comprising 3 wt% of CB-PPy exhibits similar  $G'$  and  $G''$  values over the entire frequency range thus indicating both solid-like and liquid-like behaviors. When 6 wt% of filler is added to the composite,  $G'$  is slightly higher than  $G''$ . On the other hand, the composite containing 10 wt% of CB-PPy displays a storage modulus significantly higher than the loss modulus in the whole frequency range thus indicating that the material behavior becomes more solid with the addition of conductive filler. Moreover, composites with conductive filler content lower than 3 wt% present values of  $G''$  higher than  $G'$ , representing a liquid-like behavior. On the other hand, for composites with more than 5 wt% of conductive filler,  $G'$  is higher than  $G''$  thus indicating a solid-like behavior due to the creation of a network structure in a larger degree. The rheological percolation threshold can be described by the classical percolation theory according to a power law equation (Equation 2) at the frequency of  $10^{-1}$  Hz.

$$G' = (f - f_p)^t \quad (2)$$

where  $G'$  is the storage modulus,  $f$  the filler fraction,  $f_p$  the filler fraction at the rheological percolation threshold and  $t$  a critical exponent. The rheological percolation threshold of PVDF/TPU/CB-PPy composites was found to be 3 wt% which represents the critical filler concentration that starts to create a tridimensional network that progressively hinders the movement of the polymeric chains resulting in a transition from liquid-like to solid-like behavior.

**FIGURE 5** (A) Storage and (B) complex viscosity as function of temperature for PVDF/TPU/CB-PPy conductive composites with different amounts of filler. CB-PPy, carbon black-polypyrrole; PVDF, poly(vinylidene fluoride); TPU, thermoplastic polyurethane



**FIGURE 6** Dependence of storage and loss modulus with frequency for PVDF/TPU/CB-PPy conductive composites with different amounts of filler. CB-PPy, carbon black-polypyrrole; PVDF, poly(vinylidene fluoride); TPU, thermoplastic polyurethane

### 3.2 | Electrical conductivity

The electrical conductivity of compression molded samples was measured for PVDF/TPU composites with various CB-PPy content from 0 to 15 wt% and the results are shown in Table 5.

As expected, the results indicate that the electrical conductivity of the composites increases with increasing the conductive filler. According to our previously published work,<sup>33</sup> the electrical percolation threshold of these mixtures is 5 wt% of CB-PPy. This means that in the composites with a CB-PPy content lower than 5 wt% the creation of a conductive path does not occur due to the low amount of conductive filler leading to the mixtures with electrical conductivity similar to the electrical conductivity of the neat PVDF/TPU blend. On the other hand, when the

content of CB-PPy is higher than 5 wt% there is a significant increase in the electrical conductivity of the composites due to the increase in the contact between the conductive particles that creates a conductive network in the PVDF/TPU matrix. The composites with 15 wt% of CB-PPy displays an electrical conductivity of  $3.23 \times 10^1 \text{ S}\cdot\text{m}^{-1}$ , which means an increase in the electrical conductivity of  $10^{12}$  orders of magnitude when compared to the neat PVDF/TPU blend ( $1.60 \times 10^{-11} \text{ S}\cdot\text{m}^{-1}$ ). The electrical and rheological percolation thresholds of the compression molded samples were 5 and 3 wt%, respectively.

Accordingly, to the above results, composites containing 5 and 6 wt% of filler were selected for the FFF process. These compositions were selected because they are near the electrical percolation threshold of the material and in these compositions, there are enough amount of filler to create a conductive network in the polymeric matrix.

The electrical conductivity values of the 3D printed parts are displayed in Table 6. It is possible to observe that the 3D printed specimens present lower values of electrical conductivity when compared to the compression molded samples with the same composition. The significant difference between the electrical conductivity of 3D-printed and compression molded samples can be attributed to the presence of voids in the 3D-printed parts. This behavior was also reported in the literature.<sup>35–38</sup>

### 3.3 | Microstructure

The microstructure of the cryogenically fractured surfaces of compression molded blend PVDF/TPU and composite PVDF/TPU/CB-PPy with 10 wt% of conductive filler PVDF/TPU/CB-PPy with 10% of conductive filler was evaluated by SEM and the images are displayed in

TABLE 4 Summary of main rheological properties of PVDF/TPU and PVDF/TPU/CB-PPy composites with different filler content

Sample	Viscosity at $10^{-1}$ Hz (Pa.s)	$G'$ at $10^{-1}$ Hz (Pa)	$G''$ at $10^{-1}$ Hz (Pa)
PVDF/TPU	700	2184	3816
PVDF/TPU 3%	1022	4114	4927
PVDF/TPU 5%	2647	12,556	10,910
PVDF/TPU 6%	4931	25,979	16,886
PVDF/TPU 10%	37,962	226,762	73,971

Abbreviations: CB-PPy, carbon black-polypyrrole; PVDF, poly(vinylidene fluoride); TPU, thermoplastic polyurethane.

TABLE 5 Mean electrical conductivity values with standard deviation for PVDF/TPU compression molded composites containing 0 to 15 wt% of CB-PPy

PVDF/TPU/CB-PPy compression molded	
CB-PPy (wt%)	$\sigma$ ( $S \cdot m^{-1}$ )
0	$(1.60 \pm 0.03) \times 10^{-11}$ <sup>33</sup>
3	$(3.19 \pm 0.03) \times 10^{-10}$
5	$(7.95 \pm 4.82) \times 10^{-7}$ <sup>33</sup>
6	$(1.94 \pm 1.04) \times 10^{-1}$ <sup>33</sup>
7	$(6.44 \pm 0.64) \times 10^{-1}$
10	$(5.90 \pm 0.52) \times 10^0$
15	$(3.23 \pm 0.17) \times 10^1$

Abbreviations: CB-PPy, carbon black-polypyrrole; PVDF, poly(vinylidene fluoride); TPU, thermoplastic polyurethane.

TABLE 6 Mean electrical conductivity values and standard deviation for PVDF/TPU 3D printed composites comprising 0, 5 and 6 wt% of CB-PPy<sup>33</sup>

PVDF/TPU/CB-PPy 3D printed	
CB-PPy (wt%)	$\sigma$ ( $S \cdot m^{-1}$ )
0	$(5.90 \pm 0.30) \times 10^{-12}$
5	$(9.74 \pm 7.78) \times 10^{-8}$
6	$(6.01 \pm 3.72) \times 10^{-8}$

Abbreviations: CB-PPy, carbon black-polypyrrole; PVDF, poly(vinylidene fluoride); TPU, thermoplastic polyurethane.

Figure 7. The images (A) and (B) show the phase separation where the narrows indicate the PVDF phase. This morphology was expected for immiscible polymer blends. Furthermore, Figure 7C refers to the image of the composite comprising 10 wt% of conductive filler where is possible to observe some white points that corresponds to the spherical morphology of the CB-PPy that is dispersed in the PVDF/TPU matrix).

In addition, the cross-section of cryogenically fractured 3D printed PVDF/TPU blends and of composites

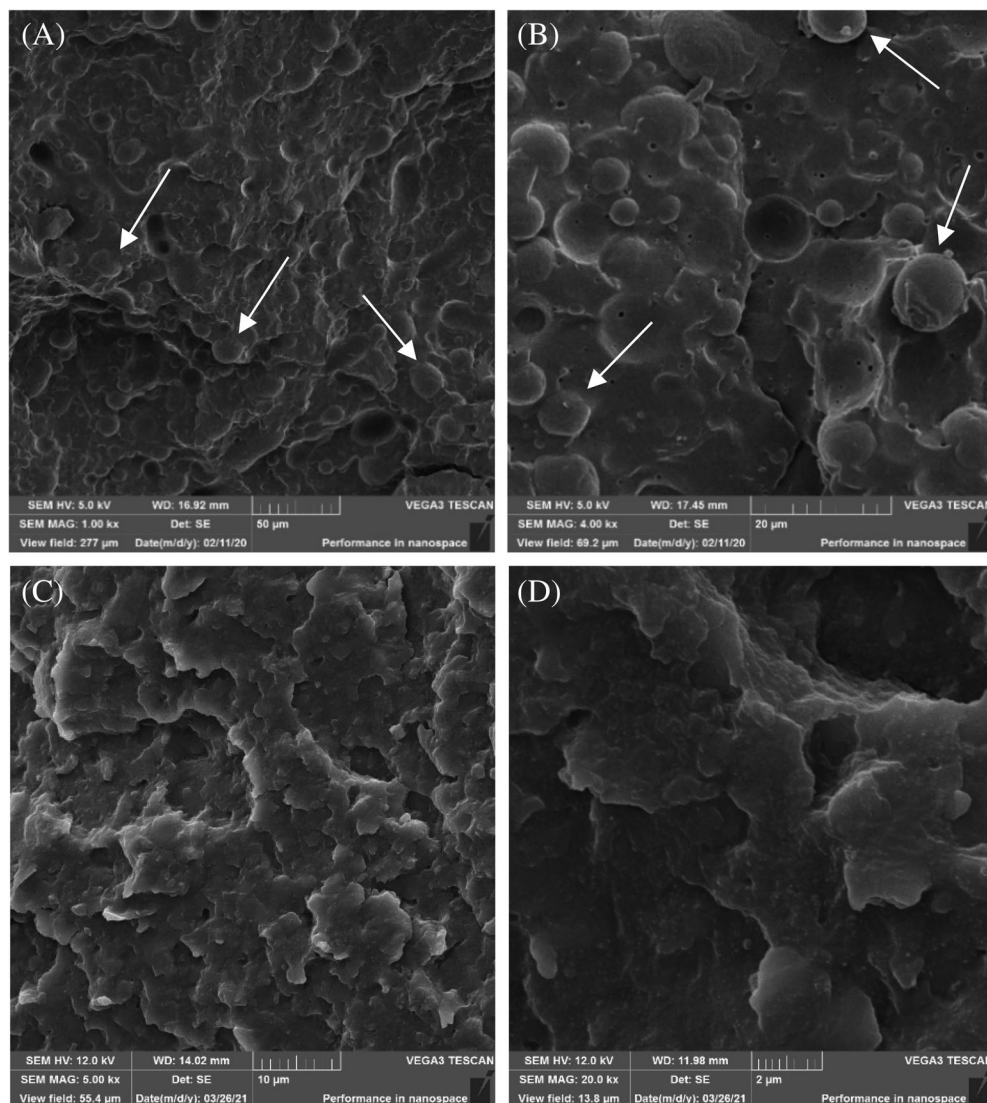
with 5 and 6 wt% are reported in Figure 8. The specimens are composed of 10 layers of 0.2 mm each deposited during the FFF process. Moreover, the images show a good adhesion between the layers. However, it is also possible to observe the presence of defects and voids between and within the layers that could explain the reduction in the electrical conductivity of 3D printed samples compared to the compression molded samples.

### 3.4 | Dynamic mechanical thermal analysis

DMTA tests were performed for PVDF/CB-PPy and TPU/CB-PPy composites containing 6% wt of conductive filler and for the composites PVDF/TPU/CB-PPy with 3, 6 and 10 wt% of filler in order to investigate the influence of the composition on the viscoelastic parameters ( $E'$  and  $\tan \delta$ ) and the glass transition temperature ( $T_g$ ) values of the composites. The DMTA curves of storage modulus and loss tangent ( $\tan \delta$ ) as a function of temperature are reported in Figure 9.

Comparing the composites with same amount of filler, it can be seen that those with a neat PVDF and neat TPU matrix display the highest and the lowest storage modulus, respectively. Thus, the addition of TPU in the blend contribute to reach more flexible materials, remarkably decreasing the storage modulus thus enhancing a desired mechanical response for flexible pressure sensors. Moreover, when comparing PVDF/TPU/CB-PPy with different filler percentages, it is possible to see that the addition of the filler increases the storage modulus of the mixtures, increasing the rigidity of the final materials. Furthermore, the  $T_g$  values were measured from the peak of the  $\tan \delta$  curves and reported in Table 7. The  $T_g$  value for PVDF/CB-PPy with 6 wt% of CB-PPy is  $-38.4^\circ\text{C}$  and it is increased to  $-33.4^\circ\text{C}$  with the addition of 50 wt% of TPU. The composite comprising TPU/CB-PPy with same amount of filler presents the lowest  $T_g$  among them with a value of  $-32.3^\circ\text{C}$ . In addition, when comparing the PVDF/TPU/CB-PPy composites, the  $T_g$  values decrease as the filler content is increased. It is important to notice

**FIGURE 7** SEM images of PVDF/TPU at (A)  $\times 1000$  and (B)  $\times 4000$  of magnification where the narrows point out the PVDF phase. SEM images of PVDF/TPU/CB-PPy 10 wt% at (C)  $\times 1000$  and (D)  $\times 20,000$  of magnification. CB-PPy, carbon black-polypyrrole; PVDF, poly(vinylidene fluoride); SEM, scanning electron microscopy; TPU, thermoplastic polyurethane



that although two  $T_g$  values are expected for immiscible polymer blends, only one is observed in PVDF/TPU composites due to the narrow temperature range between the  $T_g$  of the two neat polymers.

### 3.5 | Piezoresistive behavior

The electromechanical analysis was firstly performed for PVDF/TPU/CB-PPy composites comprising 3, 5, 6, 7, 10 and 15 wt% of conductive filler applying 2.28 MPa of compressive pressure at a rate of  $3.4 \text{ MPa} \cdot \text{min}^{-1}$  and then the pressure was released at the same rate during five loading-unloading cycles. The samples composed of PVDF/TPU and PVDF/TPU/CB-PPy 3 wt% did not manifest a piezoresistive response due to the low amount of filler content in the composite that was not enough to increase the electrical conductivity during the application of compressive stress. Composites with conductive filler

content close to the electrical percolation threshold are expected to have better electromechanical responses. The curves of compression stress and relative electrical resistance ( $R/R_0/R_0$ ) as function of time are shown in Figure 10 for the composites containing 5 and 6 wt% of CB-PPy prepared by compression molding and FFF. The application of compressive stress has a significant effect on the electrical resistivity of those composites. In fact,  $\Delta R/R_0$  substantially decreases with increasing the compressive stress indicating a certain sensitivity of the materials to the applied pressure in terms of piezoelectric response. During the application of the compressive stress, the distance between the conductive particles is reduced in the polymer matrix leading to increase the electrical conductivity of the material probably due to the tunneling resistance mechanism. Furthermore, when the compressive stress is released, the electrical resistivity of the samples returns to its initial value. On the other hand, the samples with the highest amounts of CB-PPy

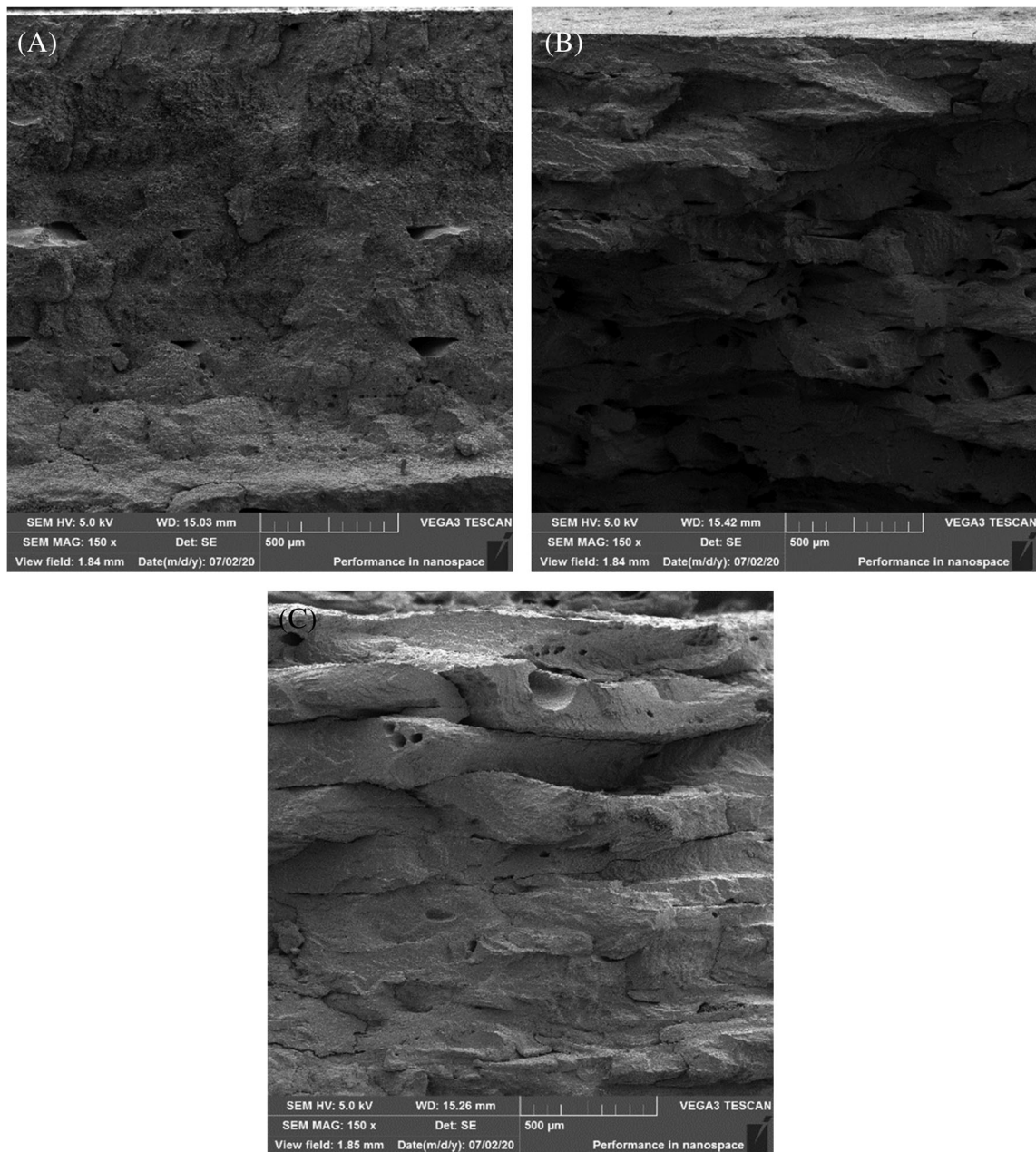


**FIGURE 8** SEM images of 3D printed specimens of (A) PVDF/TPU, (B) PVDF/TPU/CB-PPy 5 wt% and (C) PVDF/TPU/CB-PPy 6 wt% at  $\times 150$  of magnification. CB-PPy, carbon black-polyppyrole; PVDF, poly(vinylidene fluoride); SEM, scanning electron microscopy; TPU, thermoplastic polyurethane

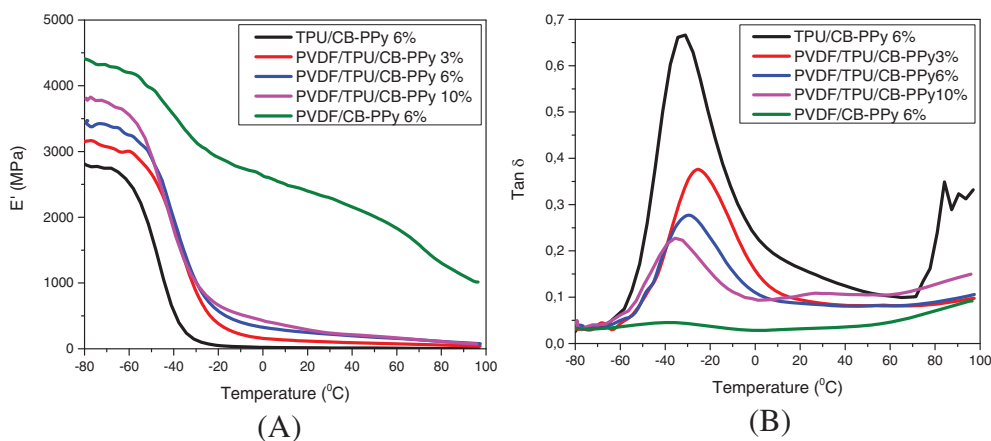


**FIGURE 9** DMTA curves of (A) storage modulus ( $E'$ ) and (B) loss tangent ( $\tan \delta$ ) as function of temperature for PVDF/CB-PPy 6%, TPU/CB-PPy 6% and PVDF/TPU/CB-PPy comprising various amounts of filler. CB-PPy, carbon black-polyppyrole; DMTA, dynamic mechanical thermal analysis; PVDF, poly(vinylidene fluoride); TPU, thermoplastic polyurethane

(7, 10 and 15 wt%) already have a conductive network in the PVDF/TPU matrix even before applying the compression stress and the stress application was not able to cause a significant change in their electrical resistivity. It is interesting to note that the piezoresistive response of the 3D printed PVDF/TPU/CB-PPy samples comprising 5 and 6 wt% of CB-PPy was similar to the response of the same materials prepared by compression molding, Figure 10, where the relative electrical resistance of the samples significantly decreases by increasing the compressive stress due to the creation of electrically conductive paths in the PVDF/TPU matrix. Also, the electrical resistivity of the samples returns to its initial value when the compressive stress is released.

The reproducibility of the piezoresistive responses were evaluated under 100 loading-unloading cycles for composites with 5 and 6 wt% of CB-PPy prepared by compression molding and FFF. The composite comprising 5 wt% of CB-PPy did not show reproducible responses

during the 100 cycles and the piezoresistive response diminished over the cycles. For the composites with 6 wt% of CB-PPy, the curves of compression stress as a function of compressive strain and piezoresistive curves for the cycles 1–10, 40–50 and 90–100 are displayed in Figure 11A–F. The stress–strain curves (Figure 11A,B) illustrate the hysteresis of the samples with 6 wt% of CB-PPy for 100 loading-unloading cycles. During the first 10 cycles, the hysteresis effect is very small, however, when comparing to 40–50 cycles and 90–100 cycles some variation of the hysteresis loops can be observed. This behavior can be assigned to the occurrence of an irreversible phenomena, such as plastic deformation in the PVDF/TPU polymeric matrix. Zheng et al claimed that the main source of hysteresis in stretchable sensors are the viscoelastic behavior of polymers and the interactions between polymers and nanomaterials.<sup>6</sup>

The curves of relative electrical resistance ( $R/R_0/R_0$ ) as a function of compressive stress and time for different cycles of composites prepared by compression molding and FFF are displayed in Figure 11C–F. As shown in Figure 11C,D, two regions corresponding the different sensitivities are identified for samples prepared by compression molding and FFF. The pressure sensitivity is related to the ability of the sensor to convert the external applied pressure into electrical signals. It can be calculated as the slope of the curves of relative electrical resistance as a function of compressive stress.<sup>39–41</sup> The first region (from 0 to 0.5 MPa) shows sensitivity of 1.4 and 1.7 kPa<sup>-1</sup> for composites prepared by compression molding and FFF, respectively. On the other hand, in the second region (from 0.5 to 2 MPa) for composites produced by compression molding and FFF shows pressure

**TABLE 7** Values of  $T_g$  for PVDF/CB-PPy 6 wt%, TPU/CB-PPy 6 wt% and PVDF/TPU/CB-PPy with different filler content

Sample	$T_g$ (°C)
PVDF/TPU	-29.4 <sup>33</sup>
PVDF/CB-PPy 6%	-38.4
PVDF/TPU/CB-PPy 3%	-28.9
PVDF/TPU/CB-PPy 6%	-33.4
PVDF/TPU/CB-PPy 10%	-35.2
TPU/CB-PPy 6%	-32.3

Abbreviations: CB-PPy, carbon black-polypyrrole; PVDF, poly(vinylidene fluoride); TPU, thermoplastic polyurethane.

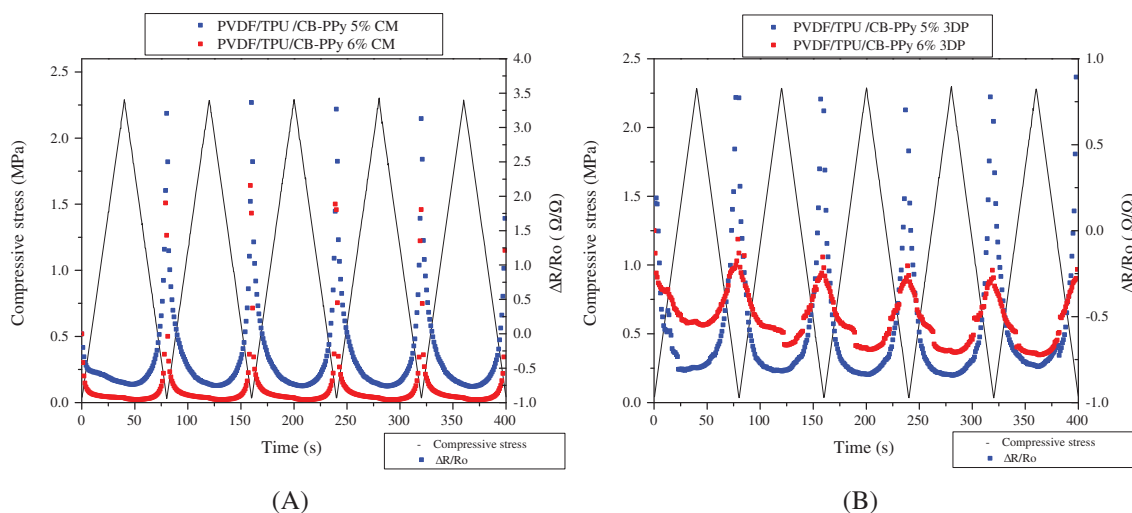


**FIGURE 10** Piezoresistive response under five loading-unloading cycles for samples of PVDF/TPU/CB-PPy comprising 5 and 6 wt% of conductive filler prepared by (A) compression molding and (B) FFF. CB-PPy, carbon black-polypyrrole; FFF, fused filament fabrication; PVDF, poly(vinylidene fluoride); TPU, thermoplastic polyurethane

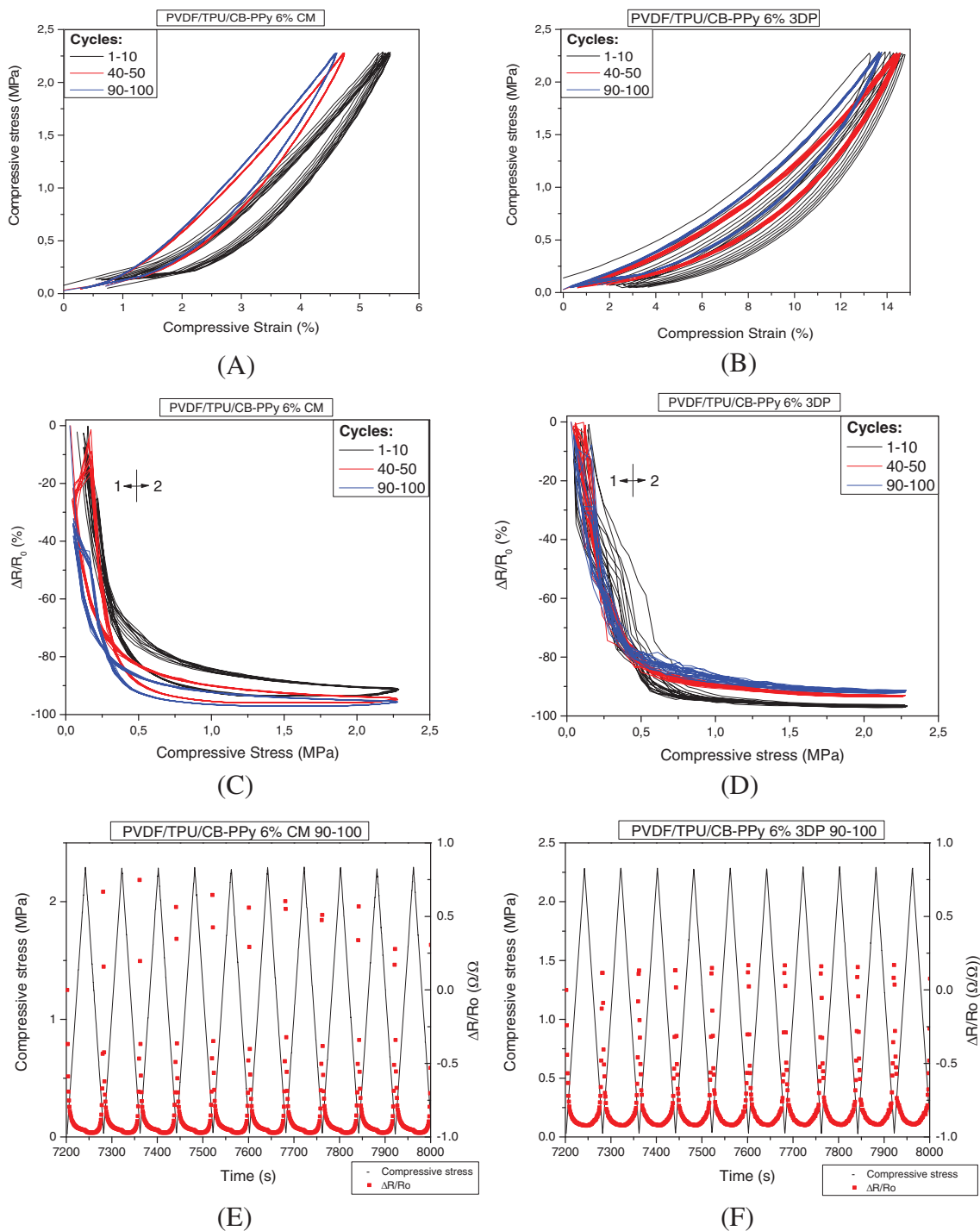


**FIGURE 11** Compressive stress–strain curves of samples prepared by (A) compression molding and (B) FFF. Relative electrical resistance ( $R-R_0/R_0$ ) versus compressive strain for samples with prepared by (C) compression molding and (D) FFF. Compressive stress and relative electrical resistance ( $R-R_0/R_0$ ) as a function of time for 90–100 cycles of samples prepared by (E) compression molding and (F) FFF. The curves are related to the PVDF/TPU/CB-PPy composites with 6 wt% of conductive filler. CB-PPy, carbon black-polypyrrole; FFF, fused filament fabrication; PVDF, poly(vinylidene fluoride); TPU, thermoplastic polyurethane

sensitivity values of  $0.05$  and  $0.04 \text{ kPa}^{-1}$ , respectively. The performance of the piezoresistive pressure sensors was also determined by the gauge factor (GF). The GF evaluates the response of the material in relation to its deformation and can be calculated by the slope of the

curves of relative electrical resistance as a function of strain.<sup>4–6,8,10,26,39–43</sup> The GF of composites prepared by compression molding and FFF were 12.8 and 18.5, respectively. The sensitivity and gauge factor values calculated for composites with 6 wt% of CB-PPy prepared by

both manufacturing methods are comparable to many other piezoresistive sensors.<sup>39–43</sup> It is important to highlighted that during the first 10 loading–unloading cycles the samples exhibit a reproducible piezoresistive response that are not significantly affected by increasing the cycles number indicating a reversible organization of the conductive path created by the conductive filler. However, those responses present a small change in their behavior for the 90 to 100 cycles, as shown in Figure 11E,F, due to the presence of some degree of plastic deformation of the matrix. Overall, the flexible composites prepared by compressing molding and FFF show high sensitivity and gauge factor, large pressure range and stable behavior indicating that FFF is also a promising fabrication method for flexible composites with good piezoresistive responses.

## 4 | CONCLUSIONS

Piezoresistive flexible pressure sensors based on PVDF/TPU filled with carbon black-polypyrrole were fabricated via compression molding and FFF. According to the rheological analysis, the addition of CB-PPy increases the storage modulus ( $G'$ ) and the complex viscosity ( $\eta^*$ ) of the composites increasing the rigidity of the material due to the formation of a 3D network. The DMTA analysis confirmed this fact since the addition of the filler increases the storage modulus of the mixtures. The rheological percolation threshold of composites was 3 wt%, which means composites with 5 or more wt% of conductive filler display  $G'$  higher than  $G''$  indicating a solid-like behavior and suggesting that the addition of higher amount of filler could compromise the processability of the composites. Moreover, the electrical conductivity of all composites increased with the increasing of filler content and the electrical percolation threshold of composites was 5 wt%. In addition, compression molded composites presented higher electrical conductivity than 3D printed specimens with same composition due to the presence of voids and defects and the presence of overlapping layers in the 3D parts that can hinder the flow of electrons.

Compression molded and 3D printed samples with 5 and 6 wt% of CB-PPy displayed good piezoresistive response. In fact, composites with conductive filler content close to the electrical percolation threshold are expected to have better electromechanical responses. However, only the composites with 6 wt% of CB-PPy showed high sensitivity and gauge factor values, large pressure range and reproducible piezoresistive responses under 100 cycles. Overall, the results indicate that the fabrication of piezoresistive flexible sensors based on

PVDF/TPU/CB-PPy composites by FFF is as promising as its fabrication by compression molding.

## ACKNOWLEDGMENTS

This research has been funded by the Italian Ministry for University and Research (MUR) through the “Departments of Excellence” program and Mayara Cristina Bertolini scholarship is funded by the “Departments of Excellence” grant L.232/2016.

## NOMENCLATURE

AM	additive manufacturing
CB	carbon black
CNT	carbon nanotubes
CPC	conductive polymeric composites
DMTA	dynamic mechanical thermal analysis
$E'$	storage modulus
$E''$	loss modulus
FFF	fused filament fabrication
$G'$	storage modulus
$G''$	loss modulus
GR	graphene
$\eta^*$	complex viscosity
PCL	polycaprolactone
PLA	polylactic acid
PMMA	poly(methyl methacrylate)
PPy	polypyrrole
PVDF	poly(vinylidene fluoride)
SEM	scanning electron microscopy
Tan $\delta$	loss tangent
$T_g$	glass transition temperature
$T_m$	melting temperature
TPU	thermoplastic polyurethane

## ORCID

Mayara C. Bertolini  <https://orcid.org/0000-0003-2852-5450>

Sithiprumnea Dul  <https://orcid.org/0000-0001-8708-6801>

Elaine C. Lopes Pereira  <https://orcid.org/0000-0001-9139-7063>

Bluma G. Soares  <https://orcid.org/0000-0002-1273-7574>

Guilherme M. O. Barra  <https://orcid.org/0000-0002-5119-0866>

Alessandro Pegoretti  <https://orcid.org/0000-0001-9641-9735>

## REFERENCES

- [1] M. Alsharari, B. Chen, W. Shu, *Proceedings* **2018**, 2, 13.
- [2] K. Ke, M. McMaster, W. Christopherson, K. D. Singer, I. Manas-Zloczower, *Compos. Part A: Appl. Sci. Manuf.* **2019**, 126, 105614.

- [3] C. Merlini, G. M. O. Barra, T. Medeiros Araujo, A. Pegoretti, *RSC Adv.* **2014**, *4*, 30.
- [4] J. R. Dios, C. Garcia-Astrain, S. Gonçalves, P. Costa, S. Lanceros-Méndez, *Compos. Sci. Technol.* **2019**, *181*, 107678.
- [5] Y. Wan, Y. Wang, C. F. Guo, *Mater Today Phys* **2017**, *1*, 61.
- [6] Q. Zheng, J.-h. Lee, X. Shen, X. Chen, J.-K. Kim, *Mater. Today* **2020**, *36*, 158.
- [7] Y. Gao, L. Yu, J. C. Yeo, C. T. Lim, *Adv. Mater.* **2020**, *32*, 15.
- [8] C. Jianwen, Z. Yutian, J. Huang, J. Zhang, D. Pan, J. Zhou, J. E. Ryu, A. Umar, Z. Guo, *Polym. Rev.* **2020**, *61*, 157.
- [9] B. Li, J. Luo, X. Huang, L. Lin, L. Wang, M. Hu, L. Tang, H. Xue, J. Gao, Y.-W. Mai, *Compos. B: Eng* **2020**, *181*, 107580.
- [10] D. Xiang, X. Zhang, Y. Li, E. Harkin-Jones, Y. Zheng, L. Wang, C. Zhao, P. Wang, *Compos. B: Eng* **2019**, *176*, 107250.
- [11] S. Muhammad Imran, Y. A. Kim, Y.-H. Choa, M. Hussain, K. S. Yang, *Polymer* **2019**, *58*, 16.
- [12] B. S. Rosa, C. Merlini, S. Livi, G. M. O. Barra, *Mater. Res.* **2019**, *22*(2), e20180541.
- [13] R. Liu, K. Xu, Y. Zhang, *Instrum. Sci. Technol.* **2020**, *48*, 4.
- [14] F. G. Souza, R. C. Michel, B. G. Soares, *Polym. Test.* **2005**, *24*, 8.
- [15] A. V. Menon, G. Madras, S. Bose, *Chem Sel* **2017**, *2*, 26.
- [16] Y. Liu, X. Yang, L. Yue, W. Li, W. Gan, K. Chen, *Polym. Compos.* **2019**, *40*, 11.
- [17] E. C. Lopes Pereira, B. G. Soares, A. A. Silva, J. M. Farias da Silva, G. M. O. Barra, S. Livi, *Polym. Test.* **2019**, *74*, 187.
- [18] B. G. Soares, L. F. Calheiros, A. A. Silva, T. Indrusiak, G. M. O. Barra, S. Livi, *J. Appl. Polym. Sci.* **2018**, *135*, 45564.
- [19] Y.-y. Shi, J.-h. Yang, T. Huang, N. Zhang, C. Chen, Y. Wang, *Compos. B: Eng* **2013**, *55*, 463.
- [20] H. Bizhani, V. Nayyeri, A. Katbab, A. Jalali-Arani, H. Nazockdast, *Eur. Polym. J.* **2018**, *100*, 209.
- [21] J. Chen, X. Cui, Y. Zhu, W. Jiang, K. Sui, *Carbon* **2017**, *114*, 441.
- [22] M. H. Al-Saleh, U. Sundararaj, *Compos. Part A: Appl. Sci. Manuf.* **2008**, *39*, 2.
- [23] U. S. M. Bera, A. Bhardwaj, P. K. Maji, *Appl Polym* **2019**, *136*, 5.
- [24] C. A. Chatham, C. E. Zawaski, D. C. Bobbitt, R. B. Moore, T. E. Long, C. B. Williams, *Macromol. Mater. Eng.* **2019**, *304*, 5.
- [25] J. A. Bencomo, S. T. Iacono, J. McCollum, *J. Mater. Chem. A* **2018**, *6*, 26.
- [26] J. F. Christ, N. Aliheidari, A. Ameli, P. Pötschke, *Mater. Des.* **2017**, *131*, 394.
- [27] Z. C. Kennedy, J. F. Christ, K. A. Evans, B. W. Arey, L. E. Sweet, M. G. Warner, R. L. Erikson, C. A. Barrett, *Nanoscale* **2017**, *9*, 17.
- [28] K. Ahmed, M. Kawakami, A. Khosla, H. Furukawa, *Polym. J.* **2019**, *51*, 5.
- [29] R. J. B. S. J. Leigh, C. P. Purcell, D. R. Billson, D. A. Hutchins, *PLoS One* **2012**, *7*, 11.
- [30] H. Kim, F. Torres, D. Villagran, C. Stewart, Y. Lin, T.-L. B. Tseng, *Macromol. Mater. Eng.* **2017**, *302*, 11.
- [31] S. Dul, A. Pegoretti, L. Fambri, *Front Mater* **2020**, *7*, 12.
- [32] S. Dul, L. Fambri, A. Pegoretti, *J. Mater. Eng. Perform.* **2021**, *30*, 5066.
- [33] M. C. Bertolini, S. Dul, G. M. O. Barra, A. Pegoretti, *J. Appl. Polym. Sci.* **2020**, *138*, 17.
- [34] E. C. Lopes Pereira, M. E. C. F. da Silva, K. Pontes, B. G. Soares, *Front Mater* **2019**, *6*, 234.
- [35] A. Dorigato, V. Moretti, S. Dul, S. H. Unterberger, A. Pegoretti, *Synth. Met.* **2017**, *226*, 7.
- [36] L. Ecco, S. Dul, D. Schmitz, G. Barra, B. Soares, L. Fambri, A. Pegoretti, *Appl. Sci.* **2019**, *9*, 1.
- [37] S. Dul, L. G. Ecco, A. Pegoretti, L. Fambri, *Polymers* **2020**, *12*, 1.
- [38] B. J. A. Gutierrez, S. Dul, A. Pegoretti, J. Alvarez-Quintana, L. Fambri, *J. Carbon Res* **2021**, *7*, 2.
- [39] P. Wei, H. Leng, Q. Chen, R. C. Advincula, E. B. Pentzer, *ACS Appl Polym Mater* **2019**, *1*, 885.
- [40] Q. Chen, P.-F. Cao, R. Advincula, *Adv. Funct. Mater.* **2018**, *28*, 1800631.
- [41] Z. Wang, X. Guan, H. Huang, H. Wang, W. Lin, Z. Peng, *Adv. Funct. Mater.* **2019**, *29*, 1807569.
- [42] E. Roh, H.-B. Lee, D.-I. Kim, N.-E. Lee, *Adv. Mater.* **2017**, *29*, 1703004.
- [43] H. B. Yao, J. Ge, C.-F. Wang, X. Wang, W. Hu, Z.-J. Zheng, Y. Ni, S.-H. Yu, *Adv. Mater.* **2013**, *29*, 1703004.

**How to cite this article:** M. C. Bertolini, S. Dul, E. C. Lopes Pereira, B. G. Soares, G. M. O. Barra, A. Pegoretti, *Polym. Compos.* **2021**, *42*(12), 6621. <https://doi.org/10.1002/pc.26327>